

AD-A134 476

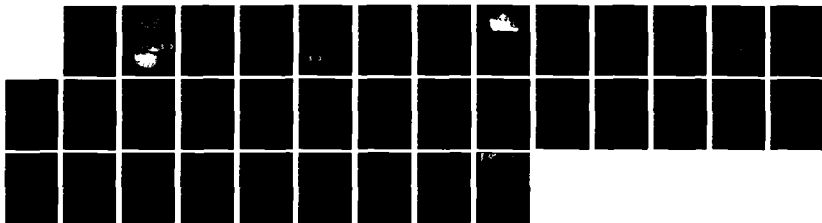
REPORTS OF THE US - USSR WEDDELL POLYNYA EXPEDITION  
OCTOBER-NOVEMBER 1981. (U) COLD REGIONS RESEARCH AND  
ENGINEERING LAB HANOVER NH E L ANDREAS ET AL. MAY 83  
CRREL-SR-83-14 NSF-DPP80-06922

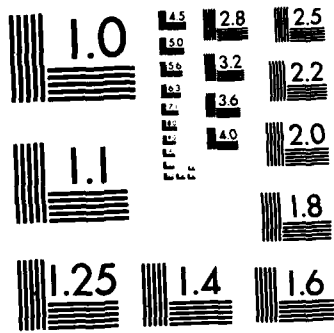
1/1

UNCLASSIFIED

F/G 4/2

NL





MICROCOPY RESOLUTION TEST CHART  
NATIONAL BUREAU OF STANDARDS-1963-A

12

AD-A134 476

Reports of the

# U.S. ~ U.S.S.R. WEDDELL POLYNYA EXPEDITION

October - November  
1981

Volume 7  
Surface-Level Meteorological Data

DTIC  
ELECTE  
NOV 8 1983  
S D B



DTIC FILE COPY

**DISTRIBUTION STATEMENT A**  
Approved for public release  
Distribution Unlimited

83 11 07 006

Unclassified

SECURITY CLASSIFICATION OF THIS PAGE (When Data Entered)

REPORT DOCUMENTATION PAGE		READ INSTRUCTIONS BEFORE COMPLETING FORM	
1. REPORT NUMBER Special Report 83-14	2. GOVT ACCESSION NO. AD-A134	3. RECIPIENT'S CATALOG NUMBER 476	
4. TITLE (and Subtitle) REPORTS OF THE U.S.-U.S.S.R. WEDDELL POLYNIA EXPEDITION, OCTOBER-NOVEMBER 1981 VOLUME 7: SURFACE-LEVEL METEOROLOGICAL DATA		5. TYPE OF REPORT & PERIOD COVERED	
		6. PERFORMING ORG. REPORT NUMBER	
7. AUTHOR(s) Edgar L. Andreas and Aleksandr P. Makshtas		8. CONTRACT OR GRANT NUMBER(s) DPP80-06922	
9. PERFORMING ORGANIZATION NAME AND ADDRESS U.S. Army Cold Regions Research and Engineering Laboratory Hanover, New Hampshire 03755		10. PROGRAM ELEMENT, PROJECT, TASK AREA & WORK UNIT NUMBERS	
11. CONTROLLING OFFICE NAME AND ADDRESS National Science Foundation Washington, D.C. 20314		12. REPORT DATE May 1983	
		13. NUMBER OF PAGES 36	
14. MONITORING AGENCY NAME & ADDRESS (If different from Controlling Office)		15. SECURITY CLASS. (of this report) Unclassified	
		15a. DECLASSIFICATION/DOWNGRADING SCHEDULE	
16. DISTRIBUTION STATEMENT (of this Report)  Approved for public release; distribution unlimited.			
17. DISTRIBUTION STATEMENT (of the abstract entered in Block 20, if different from Report)			
18. SUPPLEMENTARY NOTES			
19. KEY WORDS (Continue on reverse side if necessary and identify by block number)  Antarctic regions                      Surface-level meteorological data Marine meteorology                      Sea ice Meteorological data			
20. ABSTRACT (Continue on reverse side if necessary and identify by block number) This report summarizes a comprehensive set of surface-level meteorological data collected on the <u>Mikhail Somov</u> over sea ice in the Southern Ocean during the U.S.-U.S.S.R. Weddell Polynia Expedition in October and November of 1981. The data assembled here comprise three distinct sets of measurements: the standard meteorological observations at 3-hour intervals for 41 consecutive days, radiation and ice-surface temperature measurements every hour for 23 days while the <u>Somov</u> was within the Antarctic ice pack, and 23 sets of atmospheric surface-layer profiles of velocity, temperature and humidity for various sea-ice conditions.			

## PREFACE

Dr. Edgar L. Andreas, Physicist, Snow and Ice Branch, Research Division, U.S. Army Cold Regions Research and Engineering Laboratory, and Dr. Aleksandr P. Makshtas, Senior Scientist, Arctic and Antarctic Research Institute, Leningrad, U.S.S.R., prepared this report. The National Science Foundation supported this research with grant DPP 80-06922.

The authors thank the Soviet meteorological observers on the Mikhail Somov for making the standard meteorological observations, P.V. Bogorodskii for helping with the radiation measurements and with deployment of the profiling boom, S.F. Ackley for assisting with the surface-layer profiling, S.J. Smith and E.T. Holt for helping with the data reduction, and D.B. Clarke and J.H. Cragin for reviewing the manuscript.

The contents of this report are not to be used for advertising or promotional purposes. Citation of brand names does not constitute an official endorsement or approval of the use of such commercial products.

CONTENTS

	Page
Abstract-----	1
Preface-----	11
Introduction-----	1
Standard meteorological observations-----	2
Radiation and surface temperature measurements-----	4
Atmospheric surface-layer profiles-----	7
Literature cited-----	11
Appendix A: Standard meteorological observations-----	13
Appendix B: Radiation and surface temperature data-----	19
Appendix C: Atmospheric surface-layer profiles-----	27

ILLUSTRATIONS

Figure

1. Locations of the sensors used for the standard meteorological observations and for the radiation measurements on the <u>Mikhail Somov</u> -----	3
2. Time series of air temperature and of the ice or snow surface temperature-----	6
3. Boom assembly used for the surface-layer profiling-----	7
4. All the measured surface-layer profiles-----	10

TABLES

Table

1. Constants used for the computation of saturation vapor pressure-----	3
2. Surface-layer profiling instruments-----	8



S DTIC ELECTE D

NOV 8 1983

B

Accession For	
NTIS GRA&I	<input checked="" type="checkbox"/>
DTIC TAB	<input type="checkbox"/>
Unannounced	<input type="checkbox"/>
Justification	
By _____	
Distribution/	
Availability Codes	
Dist	Avail and/or Special
A-1	

## INTRODUCTION

The U.S.-U.S.S.R. Weddell Polynya Expedition (Gordon and Sarukhanyan 1982) collected the largest, most comprehensive set of surface-level meteorological data over Antarctic sea ice in winter since the Shackleton expedition of 1914-1917. The data set includes 41 days of standard meteorological observations, measurements of radiation components and ice-surface temperature for 23 consecutive days, and 23 sets of surface-layer wind speed, temperature and humidity profiles at select sites. This report summarizes and tabulates these data.

All of the data were collected aboard the Soviet icebreaker Mikhail Somov in October and November of 1981. Volume 1 of the set of data reports from this cruise (Huber and Gordon, in prep.) describes daily events during the expedition and, therefore, contains a map of the ship track, a chronology of all expedition observations and general remarks on navigation. To summarize the cruise very briefly: the Somov left Montevideo, Uruguay, on 9 October 1981; entered the Antarctic pack ice near latitude 56°S and longitude 3°E at about noon on 20 October; worked in the pack for 26 days, penetrating as far as latitude 62.5°S; left the ice around 9 a.m. on 14 November near latitude 57°S and longitude 0°; and returned to Montevideo on 25 November.

Ackley and Smith (1983) described sea-ice conditions during the cruise; it will likely be necessary to correlate the data that we report here with sea ice cover to interpret them unambiguously. Upper-air measurements made from the Somov during the expedition have also been tabulated (Andreas, in press). The correlation of those soundings with the data that we present here will aid in the interpretation of both data sets.

In the Standard Meteorological Observations section of this report we discuss the routine observations made on the Somov. The Radiation and Surface Temperature Measurements section contains a description of the radiation measurements made and of the important ice-surface temperature data. In the Atmospheric Surface-Layer Profiles section we describe our surface-layer profiling, the first micrometeorological measurements ever made over Antarctic sea ice at other than coastal sites.

## STANDARD METEOROLOGICAL OBSERVATIONS

The Somov's meteorological team made standard meteorological observations every 3 hours. The recorded variables include atmospheric pressure,  $P$ , wind speed,  $U$ , wind direction,  $\phi$ , air temperature,  $T_a$ , water (surface) temperature,  $T_s$ , humidity and cloud cover. We tabulate these data in Appendix A.

Figure 1 shows a photograph of the Somov with the locations of sensors indicated.  $U$  and  $\phi$  were measured with a propeller-vane mounted 23 m above the sea surface on a midship mast.  $\phi$  was measured to the nearest  $10^\circ$ ; our convention is that  $\phi$  is the direction from which the wind was blowing, with  $360^\circ$  oriented north. The components of the wind vector to the east ( $V_E$ ) and north ( $V_N$ ) are therefore

$$V_E = -U \sin\phi \quad (1)$$

$$V_N = -U \cos\phi \quad (2)$$

Wet-bulb ( $T_w$ ) and dry-bulb ( $T_a$ ) temperatures were measured on a bow boom 11 m above the sea surface (Fig. 1).  $T_w$  was converted to the dew-point temperature,  $T_d$ , using a psychrometer equation like the one given by List (1963, p. 365), and this then became the fundamental humidity variable. The saturation vapor pressure  $e_{sat}(T,P)$  (in mb) at some temperature  $T$  (in  $^\circ\text{C}$ ) and pressure  $P$  (in mb) is (Buck 1981)

$$e_{sat}(T,P) = e_0(p_b + p_a P) \exp\left[\frac{a T}{b + T}\right] \quad (3)$$

Table 1 lists the constants in eq 1; the two sets of constants refer to saturation with respect to water ( $T \geq 0^\circ\text{C}$ ) and saturation with respect to ice ( $T < 0^\circ\text{C}$ ). The vapor pressure  $e$  is simply computed from eq 3, substituting the dew point temperature  $T_d$  for  $T$ :

$$e = e_{sat}(T_d, P) \quad (4)$$

The relative humidity,  $RH$ , is defined, in turn, as

$$RH = e/e_{sat}(T_a, P) \quad (5)$$

$T_d$  and  $RH$  are the humidity variables listed in Appendix A.



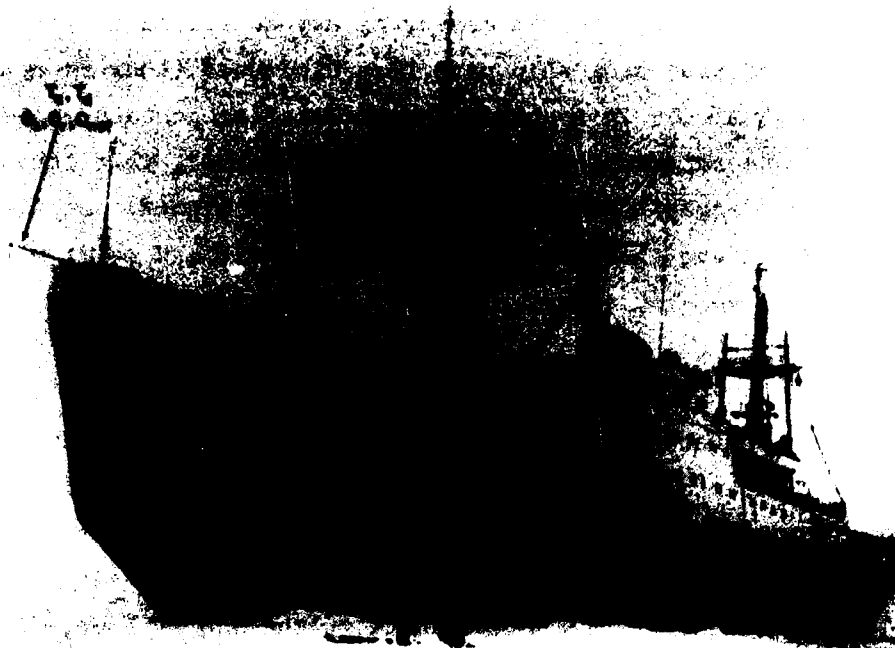


Figure 1. Locations of the sensors used for the standard meteorological observations and for the radiation measurements on the Mikhail Somov.

Table 1. Constants used in eq 3 for the computation of saturation vapor pressure.

	Over water ( $T \geq 0^{\circ}\text{C}$ )	Over ice ( $T < 0^{\circ}\text{C}$ )
$e_0$ (mb)	6.1121	6.1115
$p_a$	$3.46 \times 10^{-6}$	$4.18 \times 10^{-6}$
$p_b$ ( $\text{mb}^{-1}$ )	1.0007	1.0003
$a$	17.502	22.452
$b$ ( $^{\circ}\text{C}$ )	240.97	272.55

The uncertainties inherent in measuring any meteorological variable with instruments mounted on a ship have been discussed (Andreas et al., in review). The data listed in Appendix A may therefore contain systematic errors that we have not evaluated. We suspect, however, that these errors are generally not larger than one unit in the least significant figure. In other words, we believe that the accuracy of  $\phi$  is  $\pm 10^\circ$ ,  $U$  is  $\pm 1 \text{ m s}^{-1}$ , and  $T_a$  is  $\pm 0.1^\circ\text{C}$ , for example.

#### RADIATION AND SURFACE TEMPERATURE MEASUREMENTS

The surface temperature is a crucial parameter in the study of heat and moisture transfer across an interface. In Appendix A we list the water temperature, which would be the appropriate surface temperature in the open ocean and for low ice concentrations within the pack ice. But for more complete ice cover, the surface temperature of the ice or snow,  $T_{ice}$ , is the relevant boundary condition.

We attempted to measure  $T_{ice}$  with a thermistor protruding from a styrofoam block. We lowered this assembly from the bow of the Somov onto sea ice yet undisturbed by the ship. The block rested flat on the ice or snow surface so that the thermistor measured the temperature of a very thin surface layer. To make representative each of the hourly  $T_{ice}$  values listed in Appendix B, we sampled several floes ahead of the ship and then computed an average temperature. With this method we could make measurements when the Somov was moving as well as when it was stopped.

Thermistor temperature measurements can be affected by self-heating in the sensor. When the air temperature was near  $0^\circ\text{C}$ , we sometimes measured  $T_{ice}$  values greater than  $0^\circ\text{C}$ . Although such temperatures are thermodynamically impossible, we have retained them in Appendix B because they are suggestive. During the winter-spring transition--roughly the time of our cruise--the Antarctic ice edge is a region of dramatic ice destruction (Ackley 1979). Since thermistors seem most prone to self-heating when they make intimate thermal and physical contact with their surroundings--in our case, when the snow had a high liquid water content--we infer that the anomalously high  $T_{ice}$  values reflect melting of the snow. We may thus have been witnessing the onset of the annual Antarctic sea ice retreat.

Figure 2 shows time series of the  $T_{ice}$  values and of the air temperatures listed in Appendix A. The correlation between the two is obvious. In Figure 2 we have cut off the  $T_{ice}$  values at  $0^{\circ}\text{C}$  instead of plotting the values above  $0^{\circ}\text{C}$  given in Appendix B. There are gaps in the  $T_{ice}$  plot and in Appendix B because our method clearly did not permit a measurement of  $T_{ice}$  when the Somov happened to be surrounded by open water or ice of low concentration at the time of the hourly observations.

The bow boom (Fig. 1) had an upward-looking pyranometer for measuring the global incoming shortwave radiation,  $Q_s$ , a downward-looking pyranometer for measuring the reflected shortwave radiation,  $Q_r$ , and a net radiometer for measuring the difference between downward and upward longwave and shortwave fluxes,  $Q_{net}$ . We read these sensors every hour, too; the data are tabulated in Appendix B. Our convention is that  $Q_s$  and  $Q_r$  are always positive during daylight hours;  $Q_{net}$  is positive if the radiative flux is to the surface.

From  $Q_s$  and  $Q_r$  we calculated the shortwave albedo,

$$\alpha = 100(Q_r/Q_s) \quad (6)$$

which is also tabulated in Appendix B.  $\alpha$  values are generally between 50 and 70% but sometimes drop as low as 20%. These low values usually correspond to an absence of  $T_{ice}$  data. That is, the Somov was surrounded by mostly open water, not ice, at these times; so we would expect a low albedo.

With  $T_{ice}$  we can compute another term in the radiation budget, the emitted longwave radiation,  $Q_{L\uparrow}$ . This is

$$Q_{L\uparrow} = \epsilon \sigma T_{ice}^4 \quad (7)$$

which gives  $Q_{L\uparrow}$  in  $\text{W m}^{-2}$  for  $T_{ice}$  in K. In eq 7  $\epsilon$  is the emissivity of the sea ice, 0.97 (Andreas and Ackley 1982), and  $\sigma$  is the Stefan-Boltzmann constant,  $5.67032 \times 10^{-8} \text{ W m}^{-2} \text{ K}^{-4}$ .

The components of the radiation budget are theoretically related by

$$Q_{net} = Q_s - Q_r + Q_{L\downarrow} - Q_{L\uparrow} \quad (8)$$

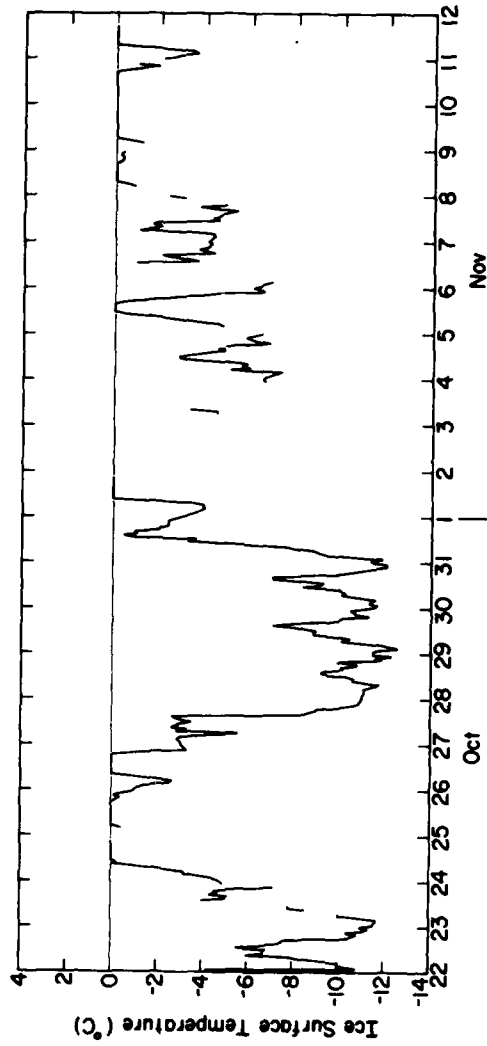
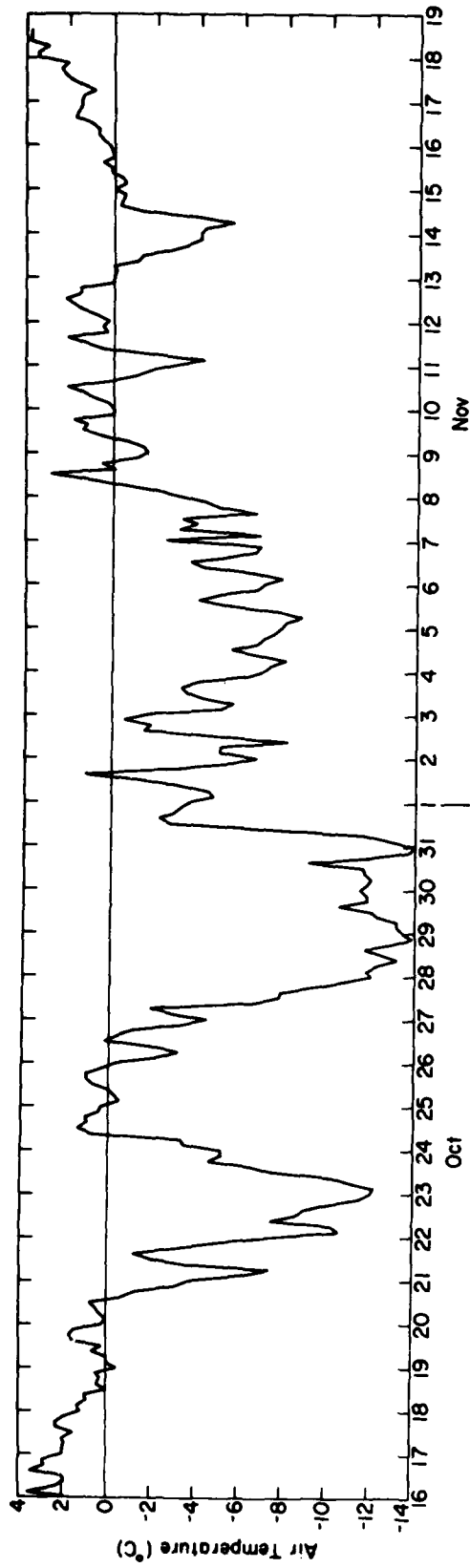


Figure 2. Time series of air temperature,  $T_a$ , from Appendix A, and of the ice or snow surface temperature,  $T_{ice}$ , from Appendix B.

where  $Q_{L\downarrow}$  is the downward flux of longwave radiation. Since we have measured or computed every term in eq 8 except  $Q_{L\downarrow}$ , we find it from

$$Q_{L\downarrow} = Q_{\text{net}} - Q_s + Q_r + Q_{L\uparrow} \quad (9)$$

These values are also listed in Appendix B.

#### ATMOSPHERIC SURFACE-LAYER PROFILES

One of the main sampling programs when the Somov stopped for station was our measurement of the atmospheric surface-layer profiles of wind velocity, temperature and humidity to study air-sea and air-ice interaction. We deployed our instruments for these measurements with a boom from the rear, starboard corner of the helicopter deck. Figure 3 is a schematic diagram of our boom assembly and shows typical sensor heights. The instrument mast on the boom had three levels of identical instrumentation for measuring wind speed, temperature and humidity; that is, we

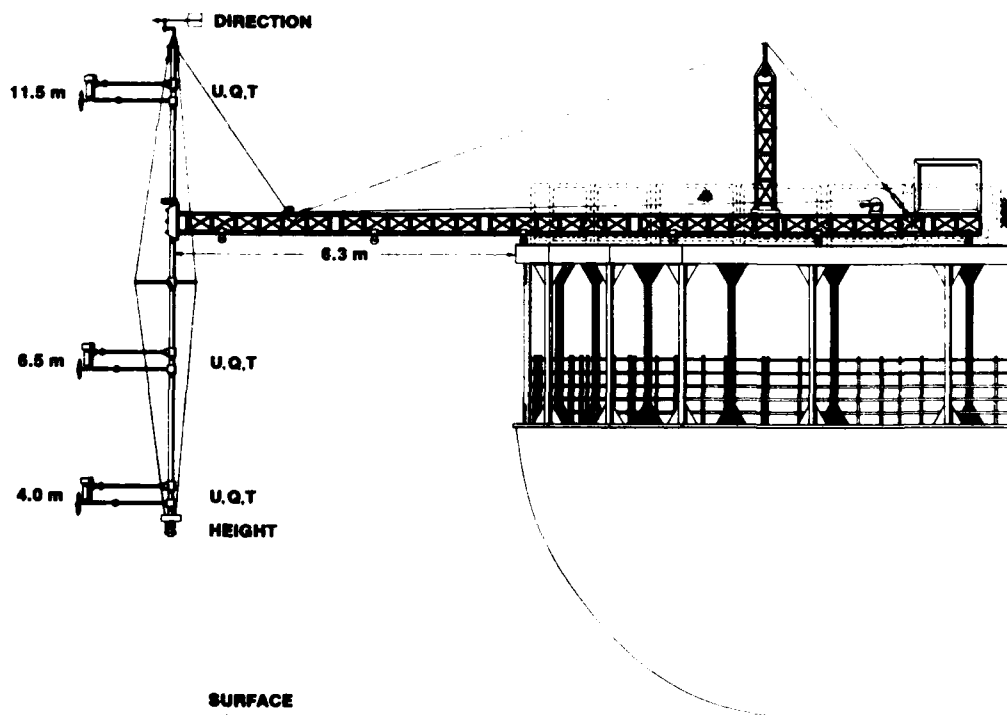


Figure 3. Boom assembly used for the surface-layer profiling, with typical sensor heights noted. U, Q and T indicate locations of velocity, humidity and temperature measurements.

Table 2. Surface-layer profiling instruments.

Variable	Sensor	Manufacturer	Model
U	Propeller anemometer	R.M. Young	27103
Direction	Vane	R.M. Young	12302
T	Platinum resistance thermometer	General Eastern	1200MPS
T <sub>d</sub>	Cooled-mirror dew-point hygrometer	General Eastern	1200MPS
Height	Sonic ranging device	Polaroid-CRREL	-

measured three-point profiles. Table 2 lists the actual instruments that were mounted on the mast. The boom assembly has been described in complete detail elsewhere (Andreas et al., in review).

When the Somov stopped for a station, the hydrographic work and biological sampling required that it be beam-into-the-wind, with the wind from starboard. Our boom, located at the rear, starboard corner of the helicopter deck, could therefore reach into the undisturbed air skirting the rear of the ship. Because the instrument mast could rotate in its central pivot assembly, we could turn the sensors directly into any wind in the rear, starboard quadrant. We used the wind vane at the top of the mast for aligning the sensors with the wind.

At the bottom of the instrument mast we mounted a sonic ranging device to use for determining the height of our instruments. The sensing element in this device was a sonic distance sensor that Polaroid uses in some of its cameras. We bought just the basic sensor from Polaroid and designed and built the housing and associated electronics at CRREL.

Appendix C summarizes the surface-layer profile data that we collected during the expedition. In particular, Table C2 lists the raw and derived data. We should, therefore, elaborate on the entries in Table C2.

The wind direction is, of course, variable over a wide range of time scales. Because the propeller anemometers have a preferred orientation, if U is the instantaneous wind speed and if these anemometers were misaligned

with this wind by a small angle  $\phi$  ( $|\phi| \leq 30^\circ$ ), they would actually show a wind speed  $U^m$  given by

$$U^m = U \cos \phi . \quad (10)$$

We recorded  $U^m$  and  $\phi$  on a strip chart and later digitized these data at 5-second intervals. We then corrected each digitized value of the measured wind speed,  $U_i^m$ , for misalignment using the digitized wind vane angle  $\phi_i$ :

$$U_i = U_i^m / \cos \phi_i . \quad (11)$$

We list the average of  $U_i$  and its sample standard deviation,  $\sigma_U$ , in Table C2. The average of  $\phi_i$ ,  $\bar{\phi}$ , is what we call in that table the wind deviation angle--the angle between the average wind vector and head-on alignment with our anemometers. When  $|\bar{\phi}|$  is small ( $\leq 30^\circ$ ), alignment was good and eq 11 is an accurate correction; when  $|\bar{\phi}|$  is larger, the correction is not as good, and the data are consequently of poorer quality.

From the measured temperature (T) profiles we computed potential temperature ( $\theta$ ) profiles from

$$\theta = T + (g/c_p)z . \quad (12)$$

Here  $z$  is the height of the measurement,  $g$  is the acceleration of gravity ( $9.819 \text{ m s}^{-2}$ ), and  $c_p$  is the specific heat of air at constant pressure ( $1.006 \times 10^3 \text{ J kg}^{-1} \text{ }^\circ\text{C}^{-1}$ ). These two temperature profiles and the sample standard deviation of  $T$ ,  $\sigma_T$ , (same for  $\theta$ ) are listed in the data table.

The humidity variable that we actually measured on the mast was the dew-point temperature  $T_d$ . This is a fundamental humidity variable because the water vapor density  $\rho_w$  can be found from it directly. That is, with  $T_d$ , we can compute the vapor pressure  $e$  from eq 4;  $\rho_w$  then comes directly from the ideal gas law (Schwerdtfeger 1976, p. 47):

$$\rho_w = M_w e / R T . \quad (13)$$

Here  $M_w$  is the molecular weight of water,  $18.0160 \times 10^{-3} \text{ kg mole}^{-1}$ , and  $R$  is the universal gas constant,  $8.31441 \text{ J mole}^{-1} \text{ }^\circ\text{C}^{-1}$ . We list both the

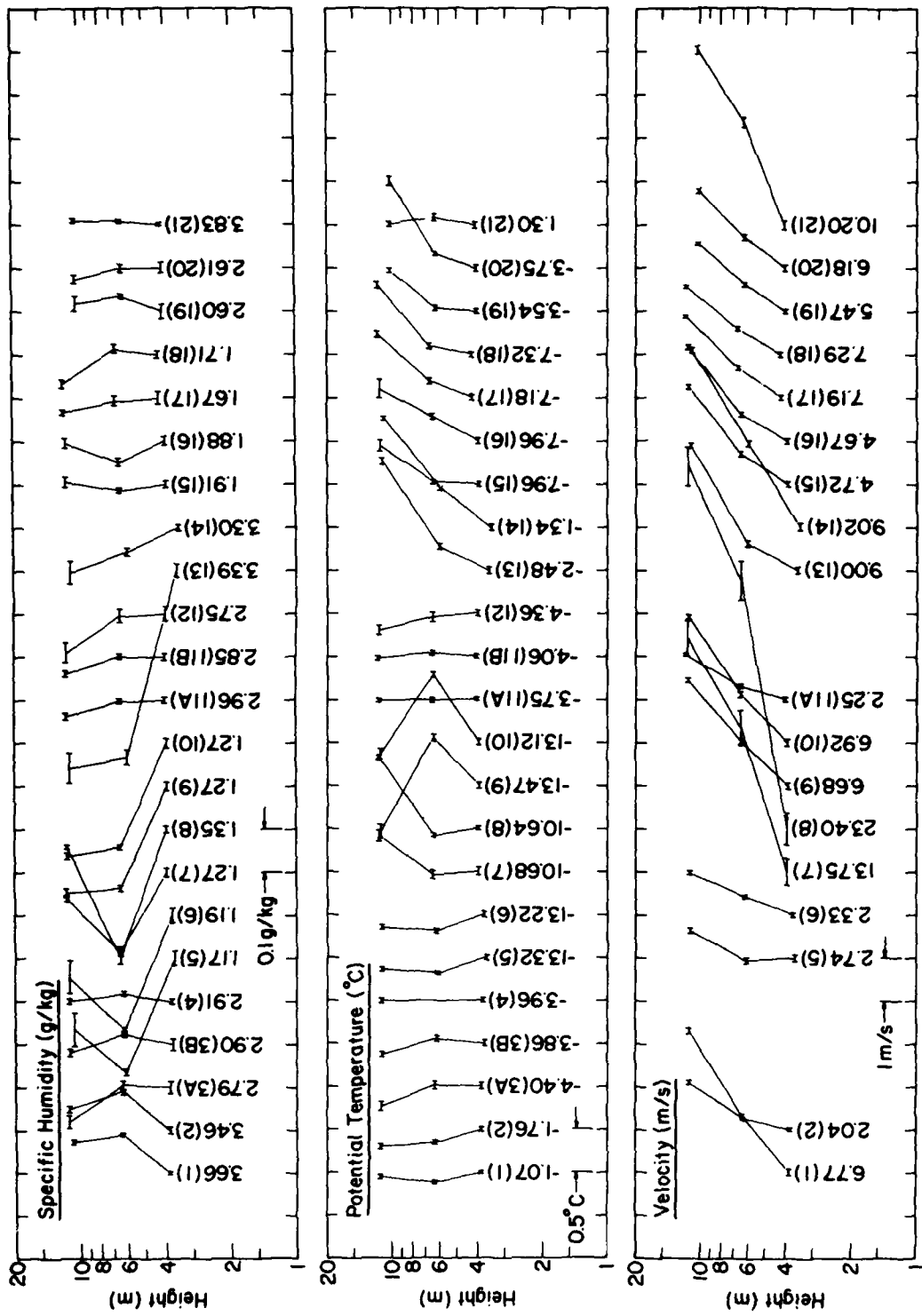


Figure 4. All the measured surface-layer profiles. The error bars are plus and minus one standard deviation. The number in parentheses under each profile is the run number; the other number is the measured value of the variable at the lowest level:  $U$  in  $m s^{-1}$ ,  $T$  in  $^{\circ}C$ , and  $Q$  in  $g kg^{-1}$ .



$T_d$  and  $\rho_w$  profiles and their sample standard deviations,  $\sigma_{T_d}$  and  $\sigma_{\rho_w}$ , in Table C2.

Most theories of the atmospheric surface layer model the specific humidity,  $Q$ , however.  $Q$  is obtained from (Pruppacher and Klett 1978, p. 77f.)

$$Q = \frac{\frac{M_w e}{M_a P}}{1 - \frac{M_w e}{M_a P}} = \frac{0.62200(e/P)}{1 - 0.37800(e/P)} \quad (14)$$

where  $M_a$  is the molecular weight of dry air,  $28.9644 \times 10^{-3}$  kg mole<sup>-1</sup>. We also include the  $Q$  profile and its sample standard deviation,  $\sigma_Q$ , in Table C2.

Figure 4 shows all the measured  $U$ ,  $\theta$  and  $Q$  profiles in chronological order. When there are missing velocity profiles, the wind was too light and variable to permit accurate measurements. We summarize the surface conditions appropriate for each profile in Appendix C. Table C1 gives the location, time and duration of each set of profiles and, thus, shows that most were recorded at night. It is consequently not surprising that the potential temperature profiles suggest that the surface layer was often stably stratified.

#### LITERATURE CITED

- Ackley, S.F. (1979) Mass-balance aspects of Weddell Sea pack ice. Journal of Glaciology, 24:391-405.
- Ackley, S.F. and S.J. Smith (1983) Reports of the U.S.-U.S.S.R. Weddell Polynya Expedition, Volume 5: Sea-Ice Observations. Hanover, New Hampshire: U.S. Army Cold Regions Research and Engineering Laboratory Special Report 83-2.
- Andreas, E.L. (in press) Reports of the U.S.-U.S.S.R. Weddell Polynya Expedition, Volume 6: Upper-Air Data. Hanover, New Hampshire: U.S. Army Cold Regions Research and Engineering Laboratory Special Report.
- Andreas, E.L. and S.F. Ackley (1982) On the differences in ablation seasons of Arctic and Antarctic sea ice. Journal of the Atmospheric Sciences, 39:440-447.

- Andreas, E.L., J.H. Rand and S.F. Ackley (in review) A simple boom assembly for the shipboard deployment of air-sea interaction instruments. Deep-Sea Research.
- Buck, A.L. (1981) New equations for computing vapor pressure and enhancement factor. Journal of Applied Meteorology, 20:1527-1532.
- Gordon, A.L. and E.I. Sarukhanyan (1982) American and Soviet expedition into the Southern Ocean sea ice in October and November 1981. Transactions, American Geophysical Union, 63:2.
- Huber, B.A. and A.L. Gordon (in prep.) Reports of the U.S.-U.S.S.R. Weddell Polynya Expedition, Volume 1: Introduction, Technical Report LDGO-2-83. Palisades, N.Y.: Lamont-Doherty Geological Observatory.
- List, R.J. (Ed.) (1963) Smithsonian Meteorological Tables, 6th Ed. Washington, D.C.: Smithsonian Institution.
- Pruppacher, H.R. and J.D. Klett (1978) Microphysics of Clouds and Precipitation. Dordrecht, Netherlands: Reidel.
- Schwerdtfeger, P. (1976) Physical Principles of Micro-Meteorological Measurements. Amsterdam, Netherlands: Elsevier.

APPENDIX A. STANDARD METEOROLOGICAL OBSERVATIONS

Definitions

- PRES . . . . surface-level atmospheric pressure
- SPEED . . . . wind speed 23 m above the surface
- DIRECTION . . direction from which the wind was blowing measured 23 m above  
the sea surface (360° is north)
- TA . . . . . air temperature 11 m above the sea surface
- TS . . . . . surface water temperature
- TD . . . . . dew-point temperature 11 m above the surface
- RH . . . . . relative humidity derived from TD
- CLOUDS . . . . cloud cover in oktas, so 8 is total cloud cover, and 9 denotes  
obscured conditions like fog, snow or darkness.



MONTH	DAY	HR (GMT)	LATITUDE (DEG S)	LONGITUDE (DEG E)	PRES (MB)	SPEED (M/S)	DIRECTION (DEGREES)	TA (C)	TS (C)	TD (C)	RH (%)	CLOUDS (OKTAS)
10	27	00	61.2	3.1	954.2	3	130	-4.5	-1.8	-6.	96.	8
10	27	03	61.2	3.1	955.7	3	20	-4.9	-1.8	-6.	95.	8
10	27	06	61.1	3.1	958.2	10	170	-5.9	-1.8	-6.	93.	8
10	27	09	61.2	3.0	959.9	9	180	-6.6	-1.8	-6.	90.	8
10	27	12	61.3	2.9	961.8	12	180	-7.8	-1.8	-6.	86.	8
10	27	15	61.3	2.9	963.5	11	200	-7.9	-1.8	-6.	83.	8
10	27	18	61.3	2.8	965.3	7	200	-9.4	-1.8	-6.	78.	8
10	27	21	61.4	2.8	966.9	13	210	-10.8	-1.8	-6.	73.	8
10	28	00	61.4	2.9	968.2	9	200	-12.0	-1.8	-	-	8
10	28	03	61.4	2.8	969.8	12	210	-11.1	-1.8	-	-	8
10	28	06	61.4	2.8	971.5	11	240	-11.1	-1.8	-	-	8
10	28	09	61.4	2.8	972.2	12	240	-11.1	-1.8	-	-	8
10	28	12	61.4	2.7	972.9	12	220	-11.1	-1.8	-	-	8
10	28	15	61.5	2.5	973.4	7	260	-11.1	-1.8	-	-	8
10	28	18	61.5	2.5	974.7	3	280	-11.1	-1.8	-	-	8
10	28	21	61.5	2.5	975.5	4	270	-11.1	-1.8	-	-	8
10	29	00	61.5	2.5	975.5	5	300	-11.3	-1.8	-	-	8
10	29	03	61.6	2.5	974.4	5	340	-11.3	-1.8	-	-	8
10	29	06	61.7	2.5	975.1	5	70	-11.3	-1.8	-	-	8
10	29	09	61.7	2.5	976.9	5	70	-11.3	-1.8	-	-	8
10	29	12	61.8	2.5	979.4	1	250	-11.3	-1.8	-	-	8
10	29	15	62.0	2.5	981.1	1	120	-11.3	-1.8	-	-	8
10	29	18	62.0	2.4	984.4	1	170	-11.3	-1.8	-	-	8
10	29	21	62.0	2.4	987.5	10	200	-11.3	-1.8	-	-	7
10	30	00	62.0	2.4	988.4	10	220	-11.5	-1.8	-	-	7
10	30	03	61.9	2.4	990.8	11	220	-11.8	-1.8	-	-	8
10	30	06	61.9	2.4	991.1	11	220	-12.0	-1.8	-	-	8
10	30	09	61.9	2.4	991.7	11	210	-11.7	-1.8	-	-	8
10	30	12	61.9	2.4	991.9	10	220	-11.7	-1.8	-	-	8
10	30	15	61.9	2.4	992.4	10	220	-11.6	-1.8	-	-	8
10	30	18	61.9	2.4	993.9	4	230	-11.9	-1.8	-	82.	8
10	30	21	61.9	2.4	995.1	8	240	-12.8	-1.8	-	-	8
10	31	00	61.9	2.4	980.2	12	10	-14.8	-1.8	-	-	8
10	31	03	62.0	2.4	973.9	13	30	-12.9	-1.8	-	-	8
10	31	06	62.0	2.4	969.8	14	40	-11.7	-1.8	-	-	8
10	31	09	62.0	2.4	966.5	11	40	-7.9	-1.8	-	91.	8
10	31	12	62.0	2.4	964.4	8	40	-2.7	-1.8	-	88.	7
10	31	15	62.0	2.4	964.4	4	20	-2.2	-1.8	-	85.	8
10	31	18	62.0	2.4	966.6	4	20	-2.9	-1.8	-	80.	8
10	31	21	62.1	2.4	967.5	5	20	-3.2	-1.8	-	83.	8
11	01	00	62.1	2.3	968.2	0	0	-3.6	-1.8	-	85.	8
11	01	03	62.1	2.3	968.9	0	20	-4.7	-1.8	-	86.	8
11	01	06	62.1	2.3	968.9	0	270	-4.5	-1.8	-	88.	8
11	01	09	62.1	2.3	970.1	5	290	-3.2	-1.8	-	87.	8
11	01	12	62.1	2.3	971.7	4	280	-1.3	-1.8	-	85.	7
11	01	15	62.1	2.3	973.9	2	290	1.2	-1.8	-	87.	7
11	01	18	62.1	2.3	975.7	2	220	-2.9	-1.8	-	84.	7
11	01	21	62.1	2.3	979.8	3	110	-5.6	-1.8	-	83.	7
11	02	00	62.2	2.2	983.0	2	150	-6.7	-1.8	-	82.	7
11	02	03	62.2	2.2	984.5	10	240	-6.0	-1.8	-	83.	8
11	02	06	62.2	2.2	987.5	10	260	-5.0	-1.8	-	83.	8
11	02	09	62.2	2.2	987.8	10	280	-8.1	-1.8	-	79.	8
11	02	12	62.2	2.2	989.9	13	350	-5.0	-1.8	-	82.	8
11	02	15	62.2	2.2	975.4	15	350	-1.5	-1.8	-	87.	8
11	02	18	62.2	2.2	972.9	15	340	-1.8	-1.8	-	82.	8
11	02	21	62.2	2.2	970.2	13	320	-0.6	-1.8	-	92.	8
11	03	00	62.3	2.1	969.5	12	300	-1.7	-1.8	-	89.	8
11	03	03	62.3	2.1	967.7	12	320	-5.0	-1.8	-	88.	8
11	03	06	62.3	2.1	963.0	11	370	-5.0	-1.8	-	79.	8
11	03	09	62.3	2.1	963.3	9	350	-3.3	-1.8	-	82.	8
11	03	12	62.3	2.1	964.5	9	250	-3.5	-1.8	-	84.	8
11	03	15	62.3	2.1	967.5	12	250	-4.6	-1.8	-	81.	8
11	03	18	62.4	2.1	968.5	12	260	-4.8	-1.8	-	78.	8
11	03	21	62.4	2.1	969.5	9	280	-6.2	-1.8	-	84.	8
11	04	00	62.4	1.9	968.9	12	280	-7.8	-1.8	-	81.	8
11	04	03	62.4	1.9	966.9	11	300	-7.3	-1.8	-	86.	8
11	04	06	62.4	1.9	966.9	11	290	-8.0	-1.8	-	90.	8
11	04	09	62.4	1.9	966.9	11	280	-6.7	-1.8	-	91.	8
11	04	12	62.4	1.9	965.9	12	290	-5.7	-1.8	-	88.	7
11	04	15	62.4	1.9	965.9	12	280	-5.7	-1.8	-	83.	8
11	04	18	62.4	1.9	965.9	9	280	-7.7	-1.8	-	80.	8
11	04	21	62.4	1.9	967.5	9	260	-7.3	-1.8	-	82.	8
11	05	00	62.5	1.8	968.3	10	260	-7.8	-1.8	-	90.	8
11	05	03	62.5	1.8	968.9	11	270	-8.0	-1.8	-	45.	8
11	05	06	62.5	1.8	969.1	10	270	-8.7	-1.8	-	89.	8
11	05	09	62.5	1.8	969.8	11	290	-7.7	-1.8	-	89.	8
11	05	12	62.5	1.8	970.8	9	290	-5.4	-1.8	-	86.	8
11	05	15	62.5	1.8	970.8	8	250	-4.0	-1.8	-	85.	8
11	05	18	62.5	1.8	972.2	10	230	-3.0	-1.8	-	86.	8
11	05	21	62.5	1.8	976.2	10	230	-6.6	-1.8	-	80.	8
11	06	00	62.5	1.7	978.7	7	220	-7.0	-1.8	-	82.	8
11	06	03	62.5	1.7	981.3	3	230	-7.8	-1.8	-	84.	8
11	06	06	62.5	1.7	983.3	3	200	-6.6	-1.8	-	86.	8
11	06	09	62.5	1.7	985.5	3	160	-4.2	-1.8	-	83.	8
11	06	12	62.5	1.7	986.5	5	240	-3.6	-1.8	-	82.	8
11	06	15	62.5	1.7	985.5	4	290	-5.4	-1.8	-	80.	8
11	06	18	62.5	1.7	985.5	8	360	-6.6	-1.8	-	83.	8
11	06	21	62.5	1.7	985.8	8	350	-6.8	-1.8	-	82.	8



MONTH	DAY	HOUR (GMT)	LATITUDE (DEG S)	LONGITUDE (DEG E)	PRES (MB)	SPEED (M/S)	DIRECTION (DEGREES)	TA (C)	TS (C)	TD (C)	RH (%)	CLOUDS (OKTAS)
11	18	00	51.2	-14.6	1017.4	19	280	3.5	1.0	1.	81.	0
11	18	03	50.9	-15.1	1017.5	16	290	3.5	2.7	1.	83.	0
11	18	06	50.8	-15.6	1016.8	12	300	3.0	2.7	0.	81.	0
11	18	09	50.5	-16.2	1016.4	12	330	3.9	3.0	1.	80.	0
11	18	12	50.4	-16.6	1014.8	15	330	3.8	1.9	1.	80.	0
11	18	15	50.1	-17.3	1010.6	11	330	3.8	1.8	1.	82.	8

APPENDIX B. RADIATION AND SURFACE TEMPERATURE DATA

Definitions

- TICE . . . . snow or ice surface temperature
- QS . . . . total sun and sky (global) radiation
- QR . . . . reflected shortwave radiation
- ALBEDO . . . shortwave albedo,  $QR/QS$
- QL-UP . . . emitted longwave radiation,  $QL_{\uparrow}$
- QL-DWN . . . incoming longwave radiation,  $QL_{\downarrow}$
- QNET . . . . net radiation or radiation balance, where a positive flux is downward, toward the surface.



MONTH	DAY	HOUR (GMT)	LATITUDE (DEG S)	LONGITUDE (DEG E)	TIME (C)	QS (W/M+2)	QR (W/M+2)	ALBEDO (%)	QL-UP (W/M+2)	QL-DWN (W/M+2)	QNET (W/M+2)
10	10	00	59	5	11	0	0	-	-	-	-20
10	10	01	59	5	11	0	0	-	-	-	-43
10	10	02	59	5	11	0	0	-	-	-	-42
10	10	03	59	5	11	0	0	-	-	-	-19
10	10	04	59	5	11	0	0	-	-	-	-12
10	10	05	59	5	11	0	0	-	-	-	17
10	10	06	59	5	11	0	0	-	-	-	16
10	10	07	59	5	11	0	0	-	-	-	40
10	10	08	59	5	11	0	0	-	-	-	70
10	10	09	59	5	11	0	0	-	-	-	142
10	10	10	59	5	11	0	0	-	-	-	183
10	10	11	59	5	11	0	0	-	-	-	240
10	10	12	59	5	11	0	0	-	-	-	255
10	10	13	59	5	11	0	0	-	-	-	78
10	10	14	59	5	11	0	0	-	-	-	98
10	10	15	59	5	11	0	0	-	-	-	40
10	10	16	59	5	11	0	0	-	-	-	22
10	10	17	59	5	11	0	0	-	-	-	2
10	10	18	59	5	11	0	0	-	-	-	-12
10	10	19	59	5	11	0	0	-	-	-	-15
10	10	20	59	5	11	0	0	-	-	-	-13
10	10	21	59	5	11	0	0	-	-	-	-14
10	10	22	59	5	11	0	0	-	-	-	-13
10	10	23	59	5	11	0	0	-	-	-	-15
10	10	00	59	4	40	0	0	-	-	-	-12
10	10	01	59	4	40	0	0	-	-	-	-11
10	10	02	59	4	40	0	0	-	-	-	-10
10	10	03	59	4	40	0	0	-	-	-	-10
10	10	04	59	4	40	0	0	-	-	-	-6
10	10	05	59	4	40	0	0	-	-	-	21
10	10	06	59	4	40	0	0	-	-	-	50
10	10	07	59	4	40	0	0	-	-	-	160
10	10	08	59	4	40	0	0	-	-	-	167
10	10	09	59	4	40	0	0	-	-	-	210
10	10	10	59	4	40	0	0	-	-	-	270
10	10	11	59	4	40	0	0	-	-	-	359
10	10	12	59	4	40	0	0	-	-	-	366
10	10	13	59	4	40	0	0	-	-	-	243
10	10	14	59	4	40	0	0	-	-	-	112
10	10	15	59	4	40	0	0	-	-	-	60
10	10	16	59	4	40	0	0	-	-	-	30
10	10	17	59	4	40	0	0	-	-	-	13
10	10	18	59	4	40	0	0	-	-	-	-17
10	10	19	59	4	40	0	0	-	-	-	-25
10	10	20	59	4	40	0	0	-	-	-	-40
10	10	21	59	4	40	0	0	-	-	-	-27
10	10	22	59	4	40	0	0	-	-	-	-18
10	10	23	59	4	40	0	0	-	-	-	-12
10	10	00	59	3	29	0	0	-	-	-	-10
10	10	01	59	3	29	0	0	-	-	-	-13
10	10	02	59	3	29	0	0	-	-	-	-2
10	10	03	59	3	29	0	0	-	-	-	0
10	10	04	59	3	29	0	0	-	-	-	7
10	10	05	59	3	29	0	0	-	-	-	22
10	10	06	59	3	29	0	0	-	-	-	30
10	10	07	59	3	29	0	0	-	-	-	65
10	10	08	59	3	29	0	0	-	-	-	98
10	10	09	59	3	29	0	0	-	-	-	159
10	10	10	59	3	29	0	0	-	-	-	180
10	10	11	59	3	29	0	0	-	-	-	280
10	10	12	59	3	29	0	0	-	-	-	320
10	10	13	59	3	29	0	0	-	-	-	308
10	10	14	59	3	29	0	0	-	-	-	245
10	10	15	59	3	29	0	0	-	-	-	70
10	10	16	59	3	29	0	0	-	-	-	68
10	10	17	59	3	29	0	0	-	-	-	70
10	10	18	59	3	29	0	0	-	-	-	45
10	10	19	59	3	29	0	0	-	-	-	20
10	10	20	59	3	29	0	0	-	-	-	5
10	10	21	59	3	29	0	0	-	-	-	0
10	10	22	59	3	29	0	0	-	-	-	0
10	10	23	59	3	29	0	0	-	-	-	0
10	10	00	59	3	30	0	0	-	-	-	0
10	10	01	59	3	30	0	0	-	-	-	0
10	10	02	59	3	30	0	0	-	-	-	0
10	10	03	59	3	30	0	0	-	-	-	0
10	10	04	59	3	30	0	0	-	-	-	0
10	10	05	59	3	30	0	0	-	-	-	-3
10	10	06	59	3	30	0	0	-	-	-	0
10	10	07	59	3	30	0	0	-	-	-	25
10	10	08	59	3	30	0	0	-	-	-	35
10	10	09	59	3	30	0	0	-	-	-	78
10	10	10	59	3	30	0	0	-	-	-	25
10	10	11	59	3	30	0	0	-	-	-	35
10	10	12	59	3	30	0	0	-	-	-	58
10	10	13	59	3	30	0	0	-	-	-	29
10	10	14	59	3	30	0	0	-	-	-	8
10	10	15	59	3	30	0	0	-	-	-	70
10	10	16	59	3	30	0	0	-	-	-	70
10	10	17	59	3	30	0	0	-	-	-	35
10	10	18	59	3	30	0	0	-	-	-	10
10	10	19	59	3	30	0	0	-	-	-	0
10	10	20	59	3	30	0	0	-	-	-	0
10	10	21	59	3	30	0	0	-	-	-	-5
10	10	22	59	3	30	0	0	-	-	-	-10
10	10	23	59	3	30	0	0	-	-	-	-10









MONTH	DAY	HOURL (GMT)	LATITUDE (DEG S)	LONGITUDE (DEG E)	TICF (C)	QS (W/M**2)	QR (W/M**2)	ALBEDO (%)	QL-UP (W/M**2)	QL-DWN (W/M**2)	QNET (W/M**2)
11	11	00	60.18	0.16	-2.00	0.0	0.0	-	297.	292.	-5.
11	11	01	60.18	0.16	-2.00	0.0	0.0	-	295.	290.	-5.
11	11	02	60.18	0.16	-2.00	0.0	0.0	-	294.	289.	-5.
11	11	03	60.18	0.16	-2.00	0.0	0.0	-	291.	276.	-5.
11	11	04	60.18	0.18	-2.00	0.0	0.0	40.	292.	287.	-5.
11	11	05	60.15	0.18	-2.00	110.	20.	40.	290.	285.	-5.
11	11	06	60.00	0.17	-2.00	110.	20.	40.	290.	285.	-5.
11	11	07	60.00	0.16	-2.00	180.	40.	40.	290.	285.	-5.
11	11	08	60.00	0.16	-2.00	220.	50.	40.	290.	285.	-5.
11	11	09	60.00	0.15	-2.00	250.	50.	40.	290.	285.	-5.
11	11	10	60.00	0.14	-2.00	250.	50.	40.	290.	285.	-5.
11	11	11	60.00	0.14	-2.00	320.	50.	40.	290.	285.	-5.
11	11	12	60.00	0.14	-2.00	350.	50.	40.	290.	285.	-5.
11	11	13	60.00	0.18	-2.00	420.	50.	40.	290.	285.	-5.
11	11	14	60.00	0.18	-2.00	420.	50.	40.	290.	285.	-5.
11	11	15	60.00	0.19	-2.00	350.	50.	40.	290.	285.	-5.
11	11	16	60.00	0.19	-2.00	350.	50.	40.	290.	285.	-5.
11	11	17	60.00	0.12	-2.00	120.	50.	40.	290.	285.	-5.
11	11	18	59.58	0.10	-2.00	120.	50.	40.	290.	285.	-5.
11	11	19	59.58	0.16	-2.00	120.	50.	40.	290.	285.	-5.
11	11	20	59.58	0.19	-2.00	120.	50.	40.	290.	285.	-5.
11	11	21	59.58	0.19	-2.00	120.	50.	40.	290.	285.	-5.
11	11	22	59.58	0.19	-2.00	120.	50.	40.	290.	285.	-5.
11	11	23	59.58	0.23	-2.00	120.	50.	40.	290.	285.	-5.
11	11	00	60.02	0.22	-2.00	0.0	0.0	-	-	-	0.
11	11	01	60.03	0.26	-2.00	0.0	0.0	-	-	-	0.
11	11	02	60.03	0.26	-2.00	0.0	0.0	-	-	-	0.
11	11	03	60.03	0.26	-2.00	0.0	0.0	-	-	-	0.
11	11	04	60.02	0.23	-2.00	45.	15.	100.	-	-	0.
11	11	05	60.04	0.24	-2.00	120.	50.	33.	-	-	15.
11	11	06	60.04	0.24	-2.00	150.	75.	50.	-	-	25.
11	11	07	60.03	0.24	-2.00	150.	75.	50.	-	-	25.
11	11	08	60.03	0.24	-2.00	150.	75.	50.	-	-	25.
11	11	09	60.03	0.24	-2.00	150.	75.	50.	-	-	25.
11	11	10	60.03	0.24	-2.00	150.	75.	50.	-	-	25.
11	11	11	60.03	0.28	-2.00	150.	75.	50.	-	-	25.
11	11	12	60.03	0.28	-2.00	150.	75.	50.	-	-	25.
11	11	13	60.03	0.31	-2.00	150.	75.	50.	-	-	25.
11	11	14	60.03	0.31	-2.00	150.	75.	50.	-	-	25.
11	11	15	60.03	0.31	-2.00	150.	75.	50.	-	-	25.
11	11	16	60.03	0.31	-2.00	150.	75.	50.	-	-	25.
11	11	17	60.03	0.31	-2.00	150.	75.	50.	-	-	25.
11	11	18	60.03	0.31	-2.00	150.	75.	50.	-	-	25.
11	11	19	60.03	0.31	-2.00	150.	75.	50.	-	-	25.
11	11	20	60.03	0.31	-2.00	150.	75.	50.	-	-	25.
11	11	21	60.03	0.31	-2.00	150.	75.	50.	-	-	25.
11	11	22	60.03	0.31	-2.00	150.	75.	50.	-	-	25.
11	11	23	60.03	0.31	-2.00	150.	75.	50.	-	-	25.
11	11	00	59.06	0.39	-2.00	0.0	0.0	-	-	-	-5.
11	11	01	59.06	0.39	-2.00	0.0	0.0	-	-	-	-5.
11	11	02	59.06	0.39	-2.00	0.0	0.0	-	-	-	-5.
11	11	03	59.06	0.39	-2.00	0.0	0.0	-	-	-	-5.
11	11	04	59.06	0.45	-2.00	40.	20.	50.	-	-	0.
11	11	05	59.06	0.45	-2.00	70.	35.	50.	-	-	10.
11	11	06	59.06	0.42	-2.00	200.	100.	50.	-	-	50.
11	11	07	59.06	0.42	-2.00	200.	100.	50.	-	-	50.
11	11	08	59.06	0.42	-2.00	200.	100.	50.	-	-	50.
11	11	09	59.06	0.41	-2.00	200.	100.	50.	-	-	50.
11	11	10	59.06	0.41	-2.00	200.	100.	50.	-	-	50.
11	11	11	59.06	0.41	-2.00	200.	100.	50.	-	-	50.
11	11	12	59.06	0.41	-2.00	200.	100.	50.	-	-	50.
11	11	13	59.06	0.48	-2.00	200.	100.	50.	-	-	50.
11	11	14	59.06	0.48	-2.00	200.	100.	50.	-	-	50.
11	11	15	59.06	0.48	-2.00	200.	100.	50.	-	-	50.
11	11	16	59.06	0.48	-2.00	200.	100.	50.	-	-	50.
11	11	17	59.06	0.48	-2.00	200.	100.	50.	-	-	50.
11	11	18	59.06	0.48	-2.00	200.	100.	50.	-	-	50.
11	11	19	59.06	0.48	-2.00	200.	100.	50.	-	-	50.
11	11	20	59.06	0.48	-2.00	200.	100.	50.	-	-	50.
11	11	21	59.06	0.48	-2.00	200.	100.	50.	-	-	50.
11	11	22	59.06	0.48	-2.00	200.	100.	50.	-	-	50.
11	11	23	59.06	0.48	-2.00	200.	100.	50.	-	-	50.

### APPENDIX C. ATMOSPHERIC SURFACE-LAYER PROFILES

We here describe the upwind surface conditions for each of the 23 surface-layer profiles listed in Tables C1 and C2.

- Runs 1, 2 . . . . 5- and 10-m floes for 100 m upwind--ice concentration was 50%. Ice concentration was 90% for the next 100 m. Continuous ice cover beyond 200 m.
- Runs 3A, 3B, 4 . Small, broken floes and slush for 50 m upwind--ice concentration 70%. Broken floes with ice coverage 100% from 50 to 150 m upwind. A continuous, flat, first-year floe beyond 150 m.
- Runs 5, 6 . . . . Small, broken floes for 200 m upwind. A uniform, flat floe beyond 200 m.
- Runs 7, 8 . . . . Open water for 30 m upwind. Smooth, unbroken ice beyond 30 m.
- Runs 9, 10 . . . . A 20-m diameter floe directly under the instrument mast. For more than 500 m upwind from this, small, broken floes of diameters 3-5 m predominated. Space between these floes filled with brash ice and slush, giving an ice concentration of more than 90%.
- Run 11A . . . . . Open water for 500 m upwind.
- Runs 11B, 12 . . . The Somov in a small polynya. Winds calm or sometimes blowing across the helicopter deck from the port side of the ship.
- Runs 13, 14 . . . . About 2 km of open water upwind.
- Runs 15, 16 . . . . The mast over open water but only 2-3 m downwind from the edge of a large, first-year floe. A 20-m-wide lead cut across this floe about 500 m upwind; beyond this more smooth ice.
- Runs 17, 18 . . . . For 300 m upwind, a few scattered, small floes with ice forming between them. Open water from 300 m to 1 km upwind. A continuous floe of first-year ice began at 1 km and continued upwind.

- Runs 19, 20 . . . . . Open water under the instrument mast and for 10 m upwind. For 75 m beyond this, thin (~ 25 cm) pancake ice and slush. From here to 700 m, larger floes (~ 50 m) of thin ice with open water between them. At 700 m a floe of first-year ice began and continued upwind.
- Run 21 . . . . . Open water with one or two larger floes (~ 50 m) for 300 m upwind. Beyond 300 m, thicker ice (~ 1 m), somewhat ridged and containing a few open water areas—concentration of this ice was 90%.

Definitions for Table C2

- PRESSURE . . . . . surface-level pressure
- WIND DEVIATION . . . . . deviation of the mean wind from head-on alignment with the anemometers
- Z . . . . . sensor height
- U . . . . . wind speed
- SIGMA-U . . . . . sample standard deviation of U
- T . . . . . temperature
- THETA . . . . . potential temperature,  $\theta$
- SIGMA-T . . . . . sample standard deviation of T and THETA
- TD . . . . . dew-point temperature,  $T_d$
- SIGMA-TD. . . . . sample standard deviation of TD
- Q . . . . . specific humidity
- SIGMA-Q . . . . . sample standard deviation of Q
- RHOW . . . . . water vapor density,  $\rho_w$
- SIGMA-RHO . . . . . sample standard deviation of RHOW.



Table C1. Chronological summary of the surface-layer profiles. The indicated radiosonde data are in Andreas (in press).

Profile						Closest radiosonde	
Date 1981	Number	Time*	Duration (min)	Latitude (S)	Longitude (E)	Time*	Number
25 October	1	2304	45	60°26.90'	3°37.07'	2348	M21
26 October	2	0056	45	60°26.90'	3°37.07'		
27 October	3A	2337	28	61°10.67'	3° 6.60'	2339	M23
	3B	0006	29	61°10.67'	3° 6.60'		
	4	0055	45	61°10.67'	3° 6.60'		
28 October	5	2304	32	61°33.02'	2°32.23'	2335	M27
29 October	6	0026	36	61°33.33'	2°33.09'		
	7	2134	46	61°57.24'	2°22.10'	2339	M29
	8	2255	45	61°57.24'	2°22.10'		
	30 October	9	2221	32	61°56.99'		
	10	2331	45	61°57.67'	2°25.41'	2335	M31
31 October	11A	2209	7	62° 5.26'	2°51.59'		
	11B	2216	38	62° 5.26'	2°51.59'	2335	M34
	12	2323	32	62° 5.24'	2°52.25'		
2 November	13	1306	31	62°15.74'	2°55.36'	1136	M37
	14	1420	33	62°16.15'	2°54.92'	1630	A13
4 November	15	2256	48	62°12.88'	1° 2.44'		
5 November	16	0023	38	62°12.61'	1° 3.00'		
6 November	17	2139	48	61°56.72'	1°12.75'	2338	M46
	18	2258	43	61°57.37'	1°12.78'		
10 November						2344	M54
11 November	19	0012	42	60°18.09'	0°16.83'	2339	M56
	20	0115	22	60°18.20'	0°16.42'		
	21	2210	47	60° 0.98'	0°19.89'		

\* Since we were so near the Greenwich Meridian, this is G.M.T. and local time.

Table C2. Atmospheric surface-layer profiles.

RUN 1 PRESSURE 951.2 MB WIND DEVIATION 55.00 DEGREES												
Z (M)	U (M/S)	SIGMA-U (M/S)	T (C)	SIGMA-T (C)	THETA (C)	TD (C)	SIGMA-TD (C)	Q (G/KG)	SIGMA-Q (G/KG)	RHOW (G/M**3)	SIGMA-RHO (G/M**3)	
3.88	6.77	0.06	-1.109	0.009	-1.071	-1.294	0.007	3.6568	0.0019	4.4471	0.0021	
6.38	7.92	0.07	-1.254	0.010	-1.192	-0.963	0.005	3.7469	0.0014	4.5588	0.0015	
11.38	9.92	0.07	-1.232	0.015	-1.121	-1.067	0.009	3.7184	0.0025	4.5238	0.0027	
RUN 2 PRESSURE 956.3 MB WIND DEVIATION 13.30 DEGREES												
Z (M)	U (M/S)	SIGMA-U (M/S)	T (C)	SIGMA-T (C)	THETA (C)	TD (C)	SIGMA-TD (C)	Q (G/KG)	SIGMA-Q (G/KG)	RHOW (G/M**3)	SIGMA-RHO (G/M**3)	
3.84	2.04	0.02	-1.798	0.020	-1.761	-2.051	0.028	3.4614	0.0072	4.2166	0.0084	
6.34	2.30	0.02	-1.976	0.021	-1.914	-1.701	0.028	3.5521	0.0073	4.3297	0.0086	
11.34	3.14	0.03	-2.067	0.023	-1.957	-1.859	0.029	3.5109	0.0075	4.2810	0.0088	
RUN 3A PRESSURE 954.2 MB WIND DEVIATION 0.00 DEGREES												
Z (M)	U (M/S)	SIGMA-U (M/S)	T (C)	SIGMA-T (C)	THETA (C)	TD (C)	SIGMA-TD (C)	Q (G/KG)	SIGMA-Q (G/KG)	RHOW (G/M**3)	SIGMA-RHO (G/M**3)	
3.83	-	-	-4.436	0.036	-4.399	-4.337	0.055	2.7859	0.0131	3.4425	0.0157	
6.33	-	-	-4.450	0.045	-4.388	-4.317	0.045	2.7906	0.0107	3.4485	0.0126	
11.33	-	-	-4.738	0.048	-4.628	-4.676	0.062	2.7065	0.0144	3.3483	0.0171	
RUN 3E PRESSURE 954.2 MB WIND DEVIATION 0.00 DEGREES												
Z (M)	U (M/S)	SIGMA-U (M/S)	T (C)	SIGMA-T (C)	THETA (C)	TD (C)	SIGMA-TD (C)	Q (G/KG)	SIGMA-Q (G/KG)	RHOW (G/M**3)	SIGMA-RHO (G/M**3)	
3.72	-	-	-3.898	0.030	-3.862	-3.869	0.054	2.8990	0.0133	3.5749	0.0160	
6.22	-	-	-3.868	0.033	-3.807	-3.774	0.027	2.9225	0.0067	3.6034	0.0078	
11.22	-	-	-4.097	0.024	-3.988	-3.945	0.033	2.8804	0.0081	3.5546	0.0096	
RUN 4 PRESSURE 953.0 MB WIND DEVIATION 0.00 DEGREES												
Z (M)	U (M/S)	SIGMA-U (M/S)	T (C)	SIGMA-T (C)	THETA (C)	TD (C)	SIGMA-TD (C)	Q (G/KG)	SIGMA-Q (G/KG)	RHOW (G/M**3)	SIGMA-RHO (G/M**3)	
3.76	-	-	-3.997	0.016	-3.960	-3.836	0.019	2.9108	0.0047	3.5862	0.0056	
6.26	-	-	-3.702	0.016	-3.641	-3.768	0.014	2.9277	0.0035	3.6299	0.0041	
11.26	-	-	-4.075	0.022	-3.965	-3.827	0.020	2.9130	0.0050	3.5900	0.0058	
RUN 5 PRESSURE 973.7 MB WIND DEVIATION -4.30 DEGREES												
Z (M)	U (M/S)	SIGMA-U (M/S)	T (C)	SIGMA-T (C)	THETA (C)	TD (C)	SIGMA-TD (C)	Q (G/KG)	SIGMA-Q (G/KG)	RHOW (G/M**3)	SIGMA-RHO (G/M**3)	
3.65	2.74	0.07	-13.358	0.025	-13.322	-13.934	0.164	1.1698	0.0177	1.5271	0.0229	
6.15	2.68	0.06	-13.567	0.011	-13.507	-16.681	0.082	0.9072	0.0070	1.1855	0.0091	
11.15	3.38	0.06	-13.568	0.021	-13.459	-15.584	0.425	1.0048	0.0403	1.3129	0.0525	
RUN 6 PRESSURE 975.5 MB WIND DEVIATION 3.30 DEGREES												
Z (M)	U (M/S)	SIGMA-U (M/S)	T (C)	SIGMA-T (C)	THETA (C)	TD (C)	SIGMA-TD (C)	Q (G/KG)	SIGMA-Q (G/KG)	RHOW (G/M**3)	SIGMA-RHO (G/M**3)	
3.72	2.33	0.03	-13.261	0.028	-13.225	-13.768	0.165	1.1855	0.0180	1.5499	0.0234	
6.22	2.75	0.03	-13.475	0.014	-13.414	-16.536	0.070	0.9179	0.0060	1.2013	0.0078	
11.22	3.31	0.03	-13.482	0.022	-13.373	-15.164	0.391	1.0427	0.0383	1.3645	0.0500	
RUN 7 PRESSURE 987.5 MB WIND DEVIATION -74.30 DEGREES												
Z (M)	U (M/S)	SIGMA-U (M/S)	T (C)	SIGMA-T (C)	THETA (C)	TD (C)	SIGMA-TD (C)	Q (G/KG)	SIGMA-Q (G/KG)	RHOW (G/M**3)	SIGMA-RHO (G/M**3)	
3.98	13.75	0.31	-10.717	0.046	-10.678	-12.846	0.089	1.2738	0.0103	1.6694	0.0132	
6.48	17.11	0.39	-10.734	0.046	-10.671	-14.551	0.094	1.0900	0.0095	1.4288	0.0121	
11.48	19.16	0.42	-10.370	0.064	-10.258	-13.376	0.055	1.2138	0.0061	1.5888	0.0076	
RUN 8 PRESSURE 987.1 MB WIND DEVIATION -76.80 DEGREES												
Z (M)	U (M/S)	SIGMA-U (M/S)	T (C)	SIGMA-T (C)	THETA (C)	TD (C)	SIGMA-TD (C)	Q (G/KG)	SIGMA-Q (G/KG)	RHOW (G/M**3)	SIGMA-RHO (G/M**3)	
3.97	23.40	0.38	-10.681	0.014	-10.642	-12.212	0.069	1.3496	0.0084	1.7678	0.0109	
6.47	29.15	0.45	-10.782	0.022	-10.719	-14.919	0.172	1.0541	0.0168	1.3814	0.0219	
11.47	31.80	0.45	-9.931	0.024	-9.819	-12.542	0.029	1.3099	0.0034	1.7109	0.0043	

RUN 9  
 PRESSURE 980.8 MB  
 WIND DEVIATION -7.70 DEGREES

Z (M)	U (M/S)	SIGMA-U (M/S)	T (C)	SIGMA-T (C)	THETA (C)	TD (C)	SIGMA-TD (C)	Q (G/KG)	SIGMA-Q (G/KG)	RHOW (G/M**3)	SIGMA-RHO (G/M**3)
3.95	6.68	0.06	-13.511	0.030	-13.472	-12.983	0.086	1.2666	0.0099	1.6665	0.0129
6.43	7.69	0.06	-12.973	0.040	-12.910	-15.227	0.061	1.0310	0.0058	1.3540	0.0074
11.45	9.13	0.05	-14.116	0.087	-14.004	-15.353	0.110	1.0191	0.0104	1.3442	0.0133

RUN 10  
 PRESSURE 979.0 MB  
 WIND DEVIATION -1.20 DEGREES

Z (M)	U (M/S)	SIGMA-U (M/S)	T (C)	SIGMA-T (C)	THETA (C)	TD (C)	SIGMA-TD (C)	Q (G/KG)	SIGMA-Q (G/KG)	RHOW (G/M**3)	SIGMA-RHO (G/M**3)
3.96	6.92	0.06	-13.160	0.029	-13.121	-12.935	0.089	1.2744	0.0103	1.6715	0.0134
6.46	8.11	0.05	-12.394	0.032	-12.331	-15.226	0.054	1.0330	0.0052	1.3511	0.0066
11.46	9.83	0.04	-13.367	0.057	-13.255	-15.433	0.079	1.0134	0.0074	1.3304	0.0095

RUN 11A  
 PRESSURE 966.3 MB  
 WIND DEVIATION -30.40 DEGREES

Z (M)	U (M/S)	SIGMA-U (M/S)	T (C)	SIGMA-T (C)	THETA (C)	TD (C)	SIGMA-TD (C)	Q (G/KG)	SIGMA-Q (G/KG)	RHOW (G/M**3)	SIGMA-RHO (G/M**3)
4.05	2.25	0.04	-3.792	0.007	-3.753	-3.907	0.026	2.9640	0.0058	3.6997	0.0071
6.55	2.56	0.03	-3.821	0.014	-3.757	-3.919	0.022	2.9613	0.0049	3.6968	0.0059
11.55	3.27	0.02	-3.877	0.012	-3.765	-4.073	0.030	2.9272	0.0066	3.6550	0.0081

RUN 11B  
 PRESSURE 966.3 MB  
 WIND DEVIATION 0.00 DEGREES

Z (M)	U (M/S)	SIGMA-U (M/S)	T (C)	SIGMA-T (C)	THETA (C)	TD (C)	SIGMA-TD (C)	Q (G/KG)	SIGMA-Q (G/KG)	RHOW (G/M**3)	SIGMA-RHO (G/M**3)
4.04	-	-	-4.097	0.013	-4.058	-4.436	0.036	2.8481	0.0078	3.5594	0.0095
6.54	-	-	-4.078	0.015	-4.014	-4.430	0.027	2.8494	0.0058	3.5608	0.0071
11.54	-	-	-4.189	0.020	-4.077	-4.609	0.032	2.8112	0.0068	3.5145	0.0082

RUN 12  
 PRESSURE 966.3 MB  
 WIND DEVIATION 0.00 DEGREES

Z (M)	U (M/S)	SIGMA-U (M/S)	T (C)	SIGMA-T (C)	THETA (C)	TD (C)	SIGMA-TD (C)	Q (G/KG)	SIGMA-Q (G/KG)	RHOW (G/M**3)	SIGMA-RHO (G/M**3)
4.00	-	-	-4.404	0.029	-4.365	-4.889	0.076	2.7522	0.0159	3.4436	0.0195
6.53	-	-	-4.463	0.035	-4.400	-4.913	0.068	2.7472	0.0142	3.4381	0.0170
11.50	-	-	-4.675	0.054	-4.563	-5.323	0.107	2.6630	0.0218	3.3355	0.0265

RUN 13  
 PRESSURE 976.8 MB  
 WIND DEVIATION -1.10 DEGREES

Z (M)	U (M/S)	SIGMA-U (M/S)	T (C)	SIGMA-T (C)	THETA (C)	TD (C)	SIGMA-TD (C)	Q (G/KG)	SIGMA-Q (G/KG)	RHOW (G/M**3)	SIGMA-RHO (G/M**3)
3.53	9.00	0.07	-2.515	0.040	-2.481	-1.942	0.059	3.3949	0.0148	4.2623	0.0180
6.63	9.61	0.07	-2.268	0.027	-2.209	-3.768	0.075	2.9629	0.0167	3.7176	0.0206
11.63	11.89	0.05	-1.321	0.028	-1.214	-3.876	0.157	2.9390	0.0349	3.6748	0.0431

RUN 14  
 PRESSURE 976.8 MB  
 WIND DEVIATION -13.60 DEGREES

Z (M)	U (M/S)	SIGMA-U (M/S)	T (C)	SIGMA-T (C)	THETA (C)	TD (C)	SIGMA-TD (C)	Q (G/KG)	SIGMA-Q (G/KG)	RHOW (G/M**3)	SIGMA-RHO (G/M**3)
3.47	9.02	0.08	-1.379	0.034	-1.345	-2.325	0.023	3.2999	0.0056	4.1260	0.0065
5.97	10.95	0.07	-0.998	0.009	-0.940	-2.549	0.058	3.2435	0.0085	4.0524	0.0104
10.97	13.11	0.06	-0.020	0.016	0.087	-2.752	0.113	3.1968	0.0270	3.9775	0.0333

RUN 15  
 PRESSURE 966.7 MB  
 WIND DEVIATION 8.90 DEGREES

Z (M)	U (M/S)	SIGMA-U (M/S)	T (C)	SIGMA-T (C)	THETA (C)	TD (C)	SIGMA-TD (C)	Q (G/KG)	SIGMA-Q (G/KG)	RHOW (G/M**3)	SIGMA-RHO (G/M**3)
3.95	4.72	0.05	-7.994	0.011	-7.956	-8.537	0.043	1.9120	0.0072	2.4269	0.0091
6.43	5.41	0.02	-7.982	0.009	-7.919	-8.623	0.032	1.8975	0.0053	2.4086	0.0067
11.43	6.96	0.05	-7.625	0.061	-7.513	-8.493	0.063	1.9194	0.0107	2.4329	0.0129

RUN 16  
 PRESSURE 966.7 MB  
 WIND DEVIATION 17.50 DEGREES

Z (M)	U (M/S)	SIGMA-U (M/S)	T (C)	SIGMA-T (C)	THETA (C)	TD (C)	SIGMA-TD (C)	Q (G/KG)	SIGMA-Q (G/KG)	RHOW (G/M**3)	SIGMA-RHO (G/M**3)
3.99	4.67	0.05	-7.997	0.024	-7.958	-8.737	0.061	1.8786	0.0101	2.3847	0.0126
6.49	5.27	0.05	-7.738	0.026	-7.675	-8.935	0.050	1.8299	0.0081	2.3207	0.0100
11.49	6.83	0.05	-7.464	0.107	-7.352	-8.756	0.070	1.8755	0.0116	2.3759	0.0137

RUN 17 PRESSURE 982.9 MB WIND DEVIATION -1.40 DEGREES												
Z (M)	U (M/S)	SIGMA-U (M/S)	T (C)	SIGMA-T (C)	THETA (C)	TD (C)	SIGMA-TD (C)	Q (G/KG)	SIGMA-Q (G/KG)	RHOW (G/M**3)	SIGMA-RHO (G/M**3)	
9.26	7.19	0.04	-7.226	0.023	-7.184	-9.878	0.009	1.6705	0.0132	2.1500	0.0168	
6.76	7.88	0.04	-7.050	0.032	-6.984	-9.935	0.065	1.6620	0.0096	2.1378	0.0121	
11.76	9.06	0.02	-6.560	0.035	-6.445	-10.093	0.026	1.6388	0.0038	2.1041	0.0046	

RUN 18 PRESSURE 982.4 MB WIND DEVIATION 15.80 DEGREES												
Z (M)	U (M/S)	SIGMA-U (M/S)	T (C)	SIGMA-T (C)	THETA (C)	TD (C)	SIGMA-TD (C)	Q (G/KG)	SIGMA-Q (G/KG)	RHOW (G/M**3)	SIGMA-RHO (G/M**3)	
9.27	7.29	0.05	-7.361	0.016	-7.319	-9.616	0.054	1.7106	0.0082	2.2016	0.0104	
6.77	7.87	0.04	-7.279	0.026	-7.213	-9.529	0.056	1.7238	0.0086	2.2179	0.0108	
11.77	8.84	0.03	-6.631	0.035	-6.516	-10.072	0.059	1.6427	0.0086	2.1086	0.0108	

RUN 19 PRESSURE 1006.5 MB WIND DEVIATION -0.60 DEGREES												
Z (M)	U (M/S)	SIGMA-U (M/S)	T (C)	SIGMA-T (C)	THETA (C)	TD (C)	SIGMA-TD (C)	Q (G/KG)	SIGMA-Q (G/KG)	RHOW (G/M**3)	SIGMA-RHO (G/M**3)	
9.07	5.47	0.04	-3.578	0.018	-3.538	-4.510	0.074	2.6828	0.0165	3.3821	0.0212	
6.31	6.09	0.04	-3.556	0.018	-3.495	-4.350	0.020	2.6385	0.0045	3.4282	0.0056	
10.31	7.03	0.03	-3.172	0.026	-3.072	-4.425	0.077	2.6217	0.0173	3.4016	0.0220	

RUN 20 PRESSURE 1006.5 MB WIND DEVIATION 8.60 DEGREES												
Z (M)	U (M/S)	SIGMA-U (M/S)	T (C)	SIGMA-T (C)	THETA (C)	TD (C)	SIGMA-TD (C)	Q (G/KG)	SIGMA-Q (G/KG)	RHOW (G/M**3)	SIGMA-RHO (G/M**3)	
9.10	6.18	0.06	-3.787	0.031	-3.747	-4.488	0.048	2.6077	0.0107	3.3911	0.0135	
6.34	6.89	0.06	-3.643	0.017	-3.581	-4.493	0.041	2.6072	0.0091	3.3887	0.0116	
10.34	7.95	0.04	-2.840	0.051	-2.739	-4.609	0.041	2.5809	0.0090	3.3445	0.0111	

RUN 21 PRESSURE 1002.0 MB WIND DEVIATION -26.10 DEGREES												
Z (M)	U (M/S)	SIGMA-U (M/S)	T (C)	SIGMA-T (C)	THETA (C)	TD (C)	SIGMA-TD (C)	Q (G/KG)	SIGMA-Q (G/KG)	RHOW (G/M**3)	SIGMA-RHO (G/M**3)	
9.15	10.20	0.10	1.264	0.032	1.304	0.065	0.007	3.8346	0.0020	4.8693	0.0019	
6.39	12.56	0.11	1.318	0.028	1.380	0.094	0.010	3.8427	0.0028	4.8786	0.0030	
10.39	14.22	0.08	1.220	0.028	1.321	0.096	0.014	3.8433	0.0039	4.8811	0.0045	

END

FINISHED

19